Proceedings of the 4th International Conference on Computing Innovation and Applied Physics
DOI: 10.54254/2753-8818/83/2025.19944

Irradiance Recovery and HDR Images Reconstruction from the Measurement of Nonlinear Response Curves of DSLR Cameras

Zunyao Wang[1,a,*]

[1]*Shenzhen College of International Education, Shenzhen, Guangdong, China*
a. Zunyaowang1110@gmail.com
**corresponding author*

Abstract: The non-linear response behavior of digital single-lens reflex cameras limits their application in scientific measurements where accurate light intensity is crucial, as pixel values in camera images do not correspond linearly to incident irradiances. This essay proposes a method for measuring the non-linear response curves of digital single-lens reflex cameras, enabling accurate recovery of incident intensities despite the inherent non-linearity of these cameras. Optimized from an existing algorithm, this technique achieves higher-quality results and faster programming times. The effectiveness and accuracy of the recovered response curve have been validated through experiments involving an optical laser setup with various incident intensities. Additionally, the response curve has been used to reconstruct high dynamic range images, yielding superior results compared to those produced directly by MATLAB functions. These findings offer a practical approach for utilizing single-lens reflex cameras with high tunability and flexibility in scientific experiments while maintaining a linear response to incident irradiance.

Keywords: Nonlinear imaging, DSLR, response curve, high dynamic range, MATLAB.

1. Research Background and Motivation

The reason that I chose this topic is related to my personal interest: photography is one of my favorite hobbies. Here is the background of the topic: a classic complementary metal-oxide-semiconductor(CMOS)/Charge-coupled Device(CCD) camera's digital sensor possesses a linear exposure-output response curve except for very few deviations at the bottom (due to noise) and top (near saturation). This means every photon the sensor receives will lead to constant brightness increments in the taken image. In contrast, digital single-lens reflex (DSLR) cameras are not linear with their logarithmic response curve designed to process images close to the photographer's observation. Despite being aesthetically pleasing, for applications that require pixel intensity information, for instance making image databases, nonlinear response curves can lead to erroneous data. Considering conventional linear CMOS/CCD cameras cannot replace DSLRs to capture high-quality pictures with multiple adjustable photographing parameters, measurement and calibration of the DSLR response curve are particularly important so as to integrate the advantages of DSLR and linear photoelectric response.

© 2025 The Authors. This is an open access article distributed under the terms of the Creative Commons Attribution License 4.0 (https://creativecommons.org/licenses/by/4.0/).

DOI: 10.54254/2753-8818/83/2025.19944

2. Research Aim

This investigation aims first to recover the nonlinear Hurter-Driffield response curve of a DSLR camera(s), then mathematically analyse it and present a fit function. The result will be compared with what has been reported in the literature and a conclusion will be proposed subsequently. In addition, the response curve will be implemented to reconstruct the corresponding high dynamic range (HDR) radiance images. The algorithm will also be compared with previous methods and commercial HDR converter software. Further investigation and applications can be added accordingly based on the research progress.

3. Literature Review

3.1. Linear and nonlinear Imaging Sensors

Linear imaging sensors, as their name suggests, generate output pixel values which are directly proportional to the incident light intensity [1]. This linear relationship enables researchers to interpret the data and apply transformations more easily to find the relationship of incident intensities between pixels. In comparison, a nonlinear sensor responds to light intensity in a way that is not proportional. For example, many consumer-grade cameras use nonlinear sensors to better capture scenes with a wide range of brightness levels and to make the image more beautiful [2]. Here, the principle of two linear imaging devices, the charge-coupled device (CCD) and complementary metal-oxide-semiconductor (CMOS), and a nonlinear imaging device, digital single-lens reflex Camera (DSLR), are illustrated in detail.

3.1.1. Charge-coupled Device and Complementary Metal-oxide-semiconductor

A CCD sensor is a type of imaging sensor that captures light and converts it into electrical charges, which are then transferred across the chip and read at one corner of the array. When photons of light hit the pixels, they are converted into electrons. Each pixel accumulates these electrons during the exposure time, with the number of electrons corresponding to the brightness of the light hitting that pixel, making the CCD a linear imaging sensor. The charges from each row of pixels are transferred vertically, one row at a time. The bottom row moves its charges into a horizontal shift register, while the other rows continue shifting their charges downward. Once in the horizontal shift register, the charges are transferred horizontally, pixel by pixel, towards the readout amplifier located at the edge of the sensor. After all the pixels have been read, the camera's processor converts the voltage signals into a digital image, which is constructed based on the intensity values from all the pixels. [3]

In comparison, a CMOS sensor is a type of imaging sensor widely used in many cameras on the market. A CMOS sensor consists of a grid of pixels that detect light, where each pixel contains a photodiode that generates an electric charge upon absorbing light, along with transistors and amplifiers that read the charge, convert it into a voltage, and send the signal for further processing. Unlike CCD sensors, which transfer charges across the entire chip to a single readout node, CMOS sensors perform processing at the pixel level, meaning the electric charges generated at each pixel are directly processed without any transfer .[4]

3.1.2. Digital Single-lens Reflex Camera

A DSLR camera is a type of digital camera that merges the mechanisms of traditional analogue single-lens reflex cameras with modern digital imaging technology. Light enters the camera through the lens, and a mirror reflects the light upwards into a pentaprism, a five-sided reflecting prism [5]. The pentaprism directs the light into the optical viewfinder, allowing the photographer to see the scene in

DOI: 10.54254/2753-8818/83/2025.19944

real-time. When the shutter button is pressed, the mirror flips up, the shutter opens, and light strikes the digital image sensor, capturing the image. The sensor converts the light into an electrical signal, which is then processed and saved as a digital image file. This is how a DSLR camera operates.

DSLR cameras offer several advantages. Due to their large sensors and the ability to use high-quality lenses, they are capable of producing high-quality images [6]. Additionally, DSLR cameras provide fast and accurate auto-focus systems, making them ideal for action photography and sports. However, DSLR cameras tend to be larger and heavier, which makes them less convenient to carry. Furthermore, the internal mirror and shutter mechanism involves moving parts that can wear out over time, potentially leading to a slight degradation in performance, such as inaccurate exposure.

3.2. Low and High Dynamic Range

Dynamic range refers to the difference between the brightest and darkest levels that a camera can capture. In imaging, it represents a sensor or camera's ability to retain details in both the shadows and highlights of a scene. High Dynamic Range (HDR) refers to imaging techniques or sensors capable of capturing a wider range of brightness levels, preserving details in both very bright and very dark areas of a scene [7]. Photographers often use HDR to capture scenes like landscapes, where both dark and bright details must be showcased. In contrast, Low Dynamic Range (LDR) refers to images or sensors that capture a narrower range of light intensity. LDR is sometimes used in older video formats to evoke a sense of nostalgia or age [8].

3.3. Response Curve Recovery

In 1997, Paul Debevec introduced a method for recovering the response curve of the imaging process and generating high dynamic range (HDR) radiance maps from photographs taken with conventional imaging equipment [7]. Debevec's technique recovers the response function that maps scene radiance to pixel values by using a series of photographs captured at different exposure times. With this response function, the algorithm fuses multiple exposures into a single HDR radiance map, where the pixel values are proportional to the true radiance of the scene.

However, Debevec's method struggles with ghosting effects in the final image. To address this, Phuoc-Hieu Le proposed a more precise approach for generating multiple exposure images from a single input image by inverting the camera response function and hallucinating missing details using neural networks [9]. When inverting the response curve, Le encountered issues with non-reversible steps, which he addressed by using convolutional neural networks (CNNs) to learn the pipeline inversion.

Further developments came in 2020 when Yu-Lun Liu proposed learning three specialized CNNs to reverse these steps: a Dequantization-Net to restore missing details in underexposed regions, a Linearization-Net to estimate the inverse camera response function (CRF) and convert the non-linear LDR image to a linear one, and a Hallucination-Net to predict missing content in overexposed regions [10]. The Dequantization-Net reduces quantization artifacts that appear as noise or contouring in smooth areas of LDR images. The Linearization-Net estimates the inverse CRF, converting the non-linear LDR image to a linear one, while the Hallucination-Net fills in missing details in overexposed regions.

In 2023, Su-Kai Chen introduced the CEVR model, which employs an implicit neural function to generate LDR images with continuous and arbitrary exposure values (EVs), including values unseen during training [11]. Chen also developed two strategies, cycle training and continuous stacking, to enhance the quality of the generated LDR stack and the final HDR reconstruction.

DOI: 10.54254/2753-8818/83/2025.19944

3.4. Debevec's Algorithm

There is a relationship between the exposure that cameras receive and the output pixel values: $Z_{ij} = f(E_i \Delta t_j)$, where Z_{ij} is the pixel value of ith pixel at jth image, E_i is the exposure received by ith pixel and Δt_j is the exposure time of jth image. By inverting the f, we can get: $f^{-1}(Z_{ij}) = E_i \Delta t_j$. Taking the natural logarithm of both sides, we can get: $\ln f^{-1}(Z_{ij}) = \ln E_i + \ln \Delta t_j$. We denote $g = \ln f^{-1}$, and therefore we have: $g(Z_{ij}) = \ln E_i + \ln \Delta t_j$. We call the function g as the response curve.

To recover the response curve g, we need to notice two characteristics of it. One is that $g(Z_{ij}) - \ln E_i - \ln \Delta t_j = 0$ and another one is $g'' = 0$, to ensure the smoothness and degree of fitness. Hence we have the function

$$O = \sum_{i=1}^{N} \sum_{j=1}^{P} [g(Z_{ij}) - \ln E_i - \ln \Delta t_j]^2 + \lambda \sum_{z=Z_{min}+1}^{z=Z_{max}-1} g''(z)^2$$

where λ is the coefficient to determine the weight of smoothness during the recovery of the response curve.

Further, we need to make three additional points to complete our description of the algorithm. First, we make an additional constraint $g(Z_{mid}) = 0$ and it means that the pixel in the middle of Z_{min} and Z_{max} has unit exposure. Second, according to our anticipation of the basic shape of the response curve, the slope will be steeper near Z_{min} and Z_{max}. The algorithm introduces a weight function $w(z)$, where

$$w(z) = \begin{cases} z - Z_{min} & \text{for} z \le \frac{1}{2}(Z_{min} + Z_{max}) \\ Z_{max} - z & \text{for} z \ge \frac{1}{2}(Z_{min} + Z_{max}) \end{cases}$$

Thirdly, The algorithm does not use every available pixel site in the solution procedure. Instead, it chooses a subset of N pixels from the P photographs, ensuring that $N(P-1) > (Z_{max} - Z_{min})$ to have a sufficiently overdetermined system.

Therefore, we have the final equation:

$$O = \sum_{i=1}^{N} \sum_{j=1}^{P} w(Z_{ij}) [g(Z_{ij}) - \ln E_i - \ln \Delta t_j]^2 + \lambda \sum_{z=Z_{min}+1}^{z=Z_{max}-1} [w(z) g''(z)]^2$$

Once we recover the response curve, we can easily convert pixel values into relative radiance values, as we know $\ln E_i = g(Z_{ij}) - \ln \Delta t_j$. To obtain a precise result, we use the weight function w again to give a higher weight to exposures in which the pixel value is closer to the middle of the response curve:

$$\ln E_i = \frac{\sum_{j=1}^{P} w(Z_{ij})(g(Z_{ij}) - \ln \Delta t_j)}{\sum_{j=1}^{P} w(Z_{ij})}$$

4. Research Method

4.1. Matrix Representation of Response Curve and Radiance Map

We define a column vector x that contains the values on the response curve and the logarithm of the radiance values:

DOI: 10.54254/2753-8818/83/2025.19944

$$x = \begin{bmatrix} g(0) \\ g(1) \\ \vdots \\ g(255) \\ \ln E_1 \\ \ln E_2 \\ \vdots \\ \ln E_N \end{bmatrix}$$

Here, $g(z)$ represents the response curve, and $\ln E_i$ represents the logarithm of the radiance for the i-th pixel.

We introduce matrices A, B, and b such that $Ax = b$. The dimensions of these matrices are defined as follows:

- A is of size $(NP + n + 1) \times (n + N)$, where N is the number of pixels per image, P is the number of images, and n is the number of possible pixel values (256 in this case).
- B is of size $N \times P$, where $B_{i,j} = \ln \Delta t_j$, with Δt_j being the exposure time of the j-th image.
- b is of size $(NP + n + 1) \times 1$.

Matrix Z contains the pixel values from the images, where Z_{ij} is the pixel value of the i-th pixel in the j-th image, ranging from 0 to 255. The first NP rows of A and b are defined as follows:

$$A_{k,Z(i,j)+1} = w(Z(i,j) + 1), \quad A_{k,n+i} = -w(Z(i,j) + 1),$$

$$b_{k,1} = w(Z(i,j) + 1) \times B_{i,j},$$

where $w(z)$ is a weighting function. The k-th row corresponds to the i-th pixel in the j-th image.

For the middle row $NP + 1$, a constraint is added to fix the response curve by setting $g(128) = 0$:

$$A_{NP+1,129} = 1, \quad b_{NP+1,1} = 0.$$

To enforce the smoothness of $g(z)$, the second derivative $g''(z)$ is considered. To derive the second derivative $g''(z)$, we start with the first derivative approximated using a forward difference: $g'(z) \approx g(z + 1) - g(z)$. Similarly, the first derivative at the previous point $z - 1$ is $g'(z - 1) \approx g(z) - g(z - 1)$. The second derivative $g''(z)$ is the difference between these two first derivatives: $g''(z) \approx g'(z) - g'(z - 1)$. Substituting the expressions for $g'(z)$ and $g'(z - 1)$, we get $g''(z) \approx [g(z + 1) - g(z)] - [g(z) - g(z - 1)]$, which simplifies to $g''(z) \approx g(z + 1) - 2g(z) + g(z - 1)$. This formula effectively captures the curvature of the function $g(z)$ using its values at adjacent points, which leads to the following entries in A for the next 254 rows:

$$A_{i,i} = \lambda \times w(i + 1), \quad A(i, i + 1) = -2 \times \lambda \times w(i + 1), \quad A(i, i + 2) = \lambda \times w(i + 1),$$

with the corresponding elements in b set to 0.

The matrices A and b take the following forms:

DOI: 10.54254/2753-8818/83/2025.19944

$$A = \begin{bmatrix} 0 & 0 & w_{1,1} & \cdots & 0 & -w_{1,1} & 0 & \cdots & 0 \\ 0 & w_{1,2} & 0 & \cdots & 0 & -w_{1,2} & 0 & \cdots & 0 \\ 0 & 0 & 0 & \cdots & w_{1,3} & -w_{1,3} & 0 & \cdots & 0 \\ \vdots & \vdots & \vdots & \vdots & \vdots & \vdots & \vdots & \vdots & \vdots \\ 0 & 0 & 0 & \cdots & w_{N,P} & 0 & 0 & \cdots & -w_{N,P} \\ 0 & 0 & \cdots & 0 & 1 & 0 & 0 & \cdots & 0 \\ \lambda \times w(2) & -2 \times \lambda \times w(2) & \lambda \times w(2) & 0 & \cdots & 0 & 0 & \cdots & 0 \\ 0 & \lambda \times w(3) & -2 \times \lambda \times w(3) & \lambda \times w(3) & 0 & \cdots & 0 & \cdots & 0 \\ 0 & 0 & \lambda \times w(4) & -2 \times \lambda \times w(4) & \lambda \times w(4) & \cdots & 0 & \cdots & 0 \end{bmatrix}$$

$$b = \begin{bmatrix} w_{1,1} \times B_{1,1} \\ w_{1,2} \times B_{2,1} \\ w_{1,3} \times B_{3,1} \\ \vdots \\ w_{1,P} \times B_{P,1} \\ \vdots \\ w_{N,1} \times B_{1,N} \\ w_{N,P} \times B_{P,N} \\ 0 \\ \vdots \\ 0 \\ 0 \\ \vdots \\ 0 \end{bmatrix}$$

By solving the equation $Ax = b$ in MATLAB, we can directly obtain the vector x. The response curve values are given by $g = x(1{:}n)$, and the radiance map is given by $\ln E = x(n+1{:}end)$.

4.2. High Dynamic Range Reconstruction

Once we recover the response curve, we can use it to reconstruct the high dynamic range (HDR) image. The reconstruction process follows this equation:

$$\ln E_i = \frac{\sum_{j=1}^{P} w\left(Z_{ij}\right)\left(g\left(Z_{ij}\right) - \ln \Delta t_j\right)}{\sum_{j=1}^{P} w\left(Z_{ij}\right)}$$

The first thing to do is to take several images of the same scene with different exposure times. Then, for each pixel in the image, apply the above equation. This will compute the actual exposure E_i at that pixel. Repeat this step for all pixels and finally we can obtain a HDR image.

4.3. Incident Intensity Recovery

To verify the accuracy of the recovered response curve, an experiment needs to be designed as follows: If we have a Gaussian beam and take photos of it, we can then reduce the beam's intensity to $\frac{1}{10}$ of its original value and take another photo. When comparing the same pixel in both images, the ratio of pixel values may not be exactly 10, as the pixel values are not linearly proportional to the actual light intensity. To address this, we use the response curve to recover the incident intensities and then compare their ratio. If the ratio is indeed 10, it indicates that the response curve has successfully recovered the true incident intensities, thereby confirming the correctness of the recovered response curve [12].

DOI: 10.54254/2753-8818/83/2025.19944

4.4. MATLAB Interpretation

In our MATLAB code, we begin by reading in the captured images. Next, we convert them into greyscale images to ensure that the pixel values represent the average of all three colour channels. Following this, we create matrices and process the pixel values according to the previously discussed procedure. Once these steps are completed, we can derive the response curve for our DSLR camera. The detailed procedure can be seen in **Algorithm 1**.

Algorithm 1 Response Curve Recovery

Read Image1, Image2, Image3, …Image20 from the specified path
Convert Image1, Image2, …Image20 to grayscale and store in I_1, I_2, …I_{20} ,respectively
$n \leftarrow Numberofpixelsselected$
$p \leftarrow Numberofimages$
$\lambda \leftarrow aspecificvalue$
$Z \leftarrow$ zeros of size (n, p)
$B \leftarrow$ zeros of size (n, p)
$w \leftarrow$ zeros of size $(1{,}256)$
for $i = i$ **to** n **do**
  Randomly select a pixel
  for $j = i$ **to** p **do**
    Store grayscale pixel value of the selected pixel in $Z(i, j)$
    Store corresponding log exposure time in $B(i, j)$
  end for
end for
for z $= 0$ **to** 255 **do**
  if z ≤ 127.5 **then**
    $w(z + 1) \leftarrow z$
  else
    $w(z + 1) \leftarrow 255 - z$
  end if
end for
Initialize matrix A with dimensions $\big((n \times p) + (256 - 1), 256 + n\big)$
Initialize vector b with size equal to the number of rows in A
$k \leftarrow 1$
for i =1 **to** n **do**
  for j =1 **to** p **do**
    $w_{ij} \leftarrow w(Z(i, j) + 1)$
    Fill $A(k, Z(i, j) + 1)$ with w_{ij} and $A(k, 256 + i)$ with $-w_{ij}$
    $b(k) \leftarrow w_{ij} \cdot B(i, j)$
    $k \leftarrow k + 1$
  end for
end for
Set $A(k, 129) = 1$

$k \leftarrow k + 1$
for i =1 **to** 254 **do**
  Add smoothness constraint to A using weights
  $k \leftarrow k + 1$

DOI: 10.54254/2753-8818/83/2025.19944

end for
Solve $x = A\backslash b$
$g \leftarrow x(1{:}256)$
$lE \leftarrow x(257{:}end)$

The next step is HDR image reconstruction. To reconstruct the HDR image, we first recover the response curves for each of the RGB channels. We then input several images to be reconstructed. For each RGB channel, we recover the actual exposure using the corresponding response curve. Finally, we combine the three HDR images from each RGB channel to generate a complete HDR image. The detailed procedure is outlined in **Algorithm 2**).

Algorithm 2 HDR Reconstruction

Define $numNewImages =$ number of new image to be combined into HDR
Initialize I_new to store new images
for i =1 **to** *numNewImages* **do**
  Read new image from the specified path and store in $I_new[i]$
end for
  Set $B_new = \log$(new shutter speeds)
for c =1 to 3 **do**
  Initialize $E_new[c]$ as a matrix of zeros
  for i =1 to number of roes in $E_new[c]$ **do**
    for j =1 to number of roes in $E_new[c]$ **do**
      Initialize $sum1 = 0$, $sum2 = 0$
      for k =1 to numNewImages **do**
        Get pixel value from $I_new[k](i, j, c)$
        Update $sum1$ and $sum2$ using weight w and response curve g
      end for
      Set $E_new[c](i, j) = \exp(sum1/sum2)$
    end for
  end for
end for
Combine $E_new[1]$, $E_new[2]$, and $E_new[3]$ into hdr_image_new
Apply tone mapping to hdr_image_new and store in I_final_new
Display I_final_new

5. Experimental Results

The expected results are that we obtain the response curve and radiance map of the image. We will then use the response curve to mix several images into an HDR image.

5.1. Response Curve Recovery

Based on the provided algorithm, we have edited the MATLAB code and captured images to recover the response curve. The process involves taking multiple photographs of the same scene with varying exposure times, which serve as input to the MATLAB code. The code processes these images by extracting the pixel values and applying the specified mathematical model to recover the response curve. This curve allows us to accurately map pixel values to scene radiance, ensuring that the camera's response to light is correctly characterised.

DOI: 10.54254/2753-8818/83/2025.19944

5.1.1. Attempt and Review

The response curves in figure 1 were recovered from the calibration images in figure 2. It is clear that both response curves exhibit an anomalous turning point around a pixel value of 250. This anomaly is caused by the reflection of light from the surface of the insecticide tank. The reflection creates regions of significantly higher brightness compared to the rest of the scene, introducing a high dynamic range element. This not only makes it challenging to achieve consistent exposure across the different images but also leads to overexposed or saturated pixels if the exposure is not adjusted properly. As a result, the weighting function used in the response curve recovery is affected, as the bright, reflective areas disproportionately influence the recovered curve.

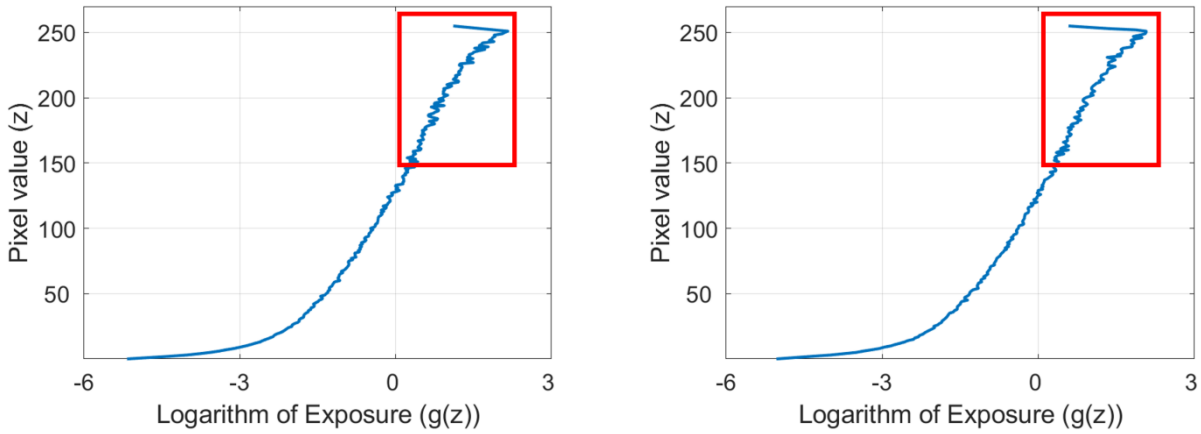

Figure 1: The response curve of image 5.2, where the left has a $\lambda = 0.1$ and the right has a $\lambda = 1$

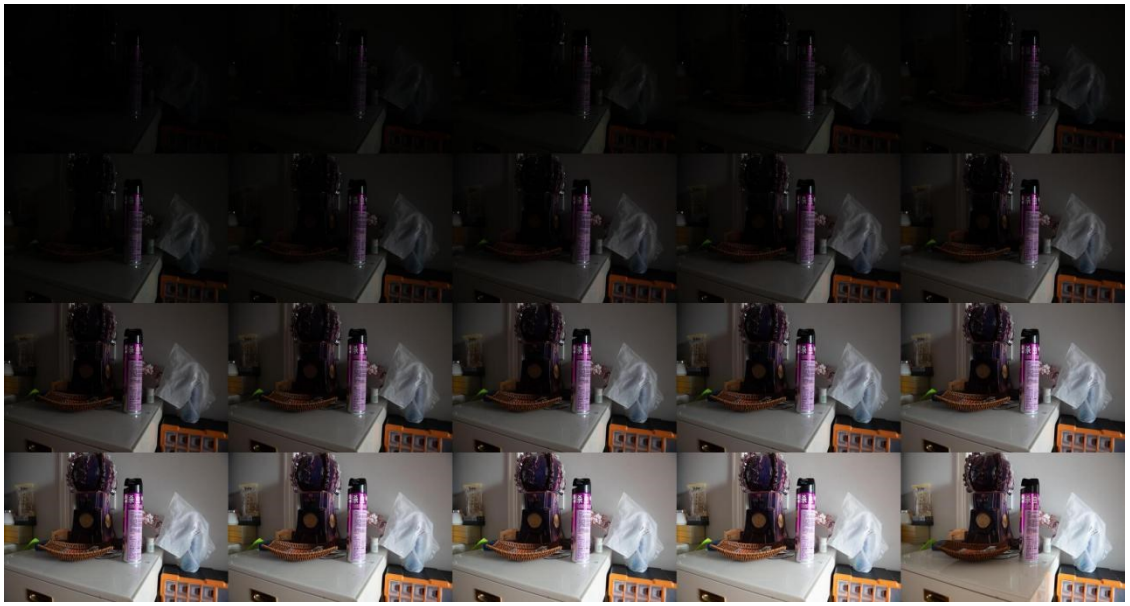

Figure 2: The sets of image depicts a cluttered tabletop with various items, including a decorative vase, a insecticide tank and a clear plastic bag

Another scene worth discussing is shown in figure 3. The presence of too many details in the image can significantly affect the recovery of the camera response curve. A high density of details increases local contrast, making it harder to measure the response curve accurately since pixel values fluctuate significantly over small regions. Additionally, reflective surfaces like glossy book covers and metallic figurines alter light in a non-linear manner, further complicating the extraction of the response curve.

DOI: 10.54254/2753-8818/83/2025.19944

To mitigate this issue, a large number of pixels are required, which increases the computational load. As shown in figure 4, using $n = 1000$ pixels results in a rough response curve, while a relatively smooth curve is achieved with $n = 5000$ pixels. However, the longer compilation time for $n = 5000$ highlights the inefficiency of this approach.

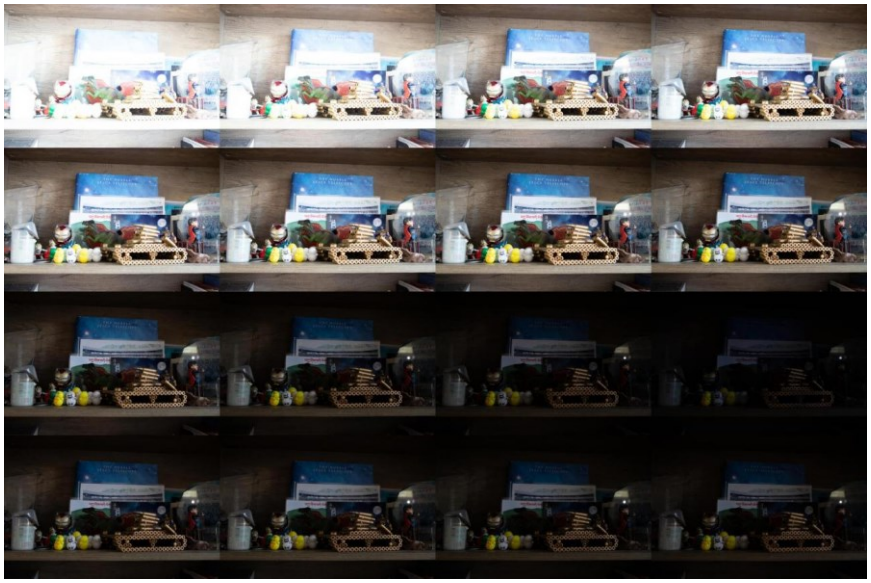

Figure 3: This image depicts a cluttered shelf filled with various objects including a book titled "THE HUBBLE SPACE TELESCOPE" with a starry sky cover at the background, some toys, figurines and decorative items

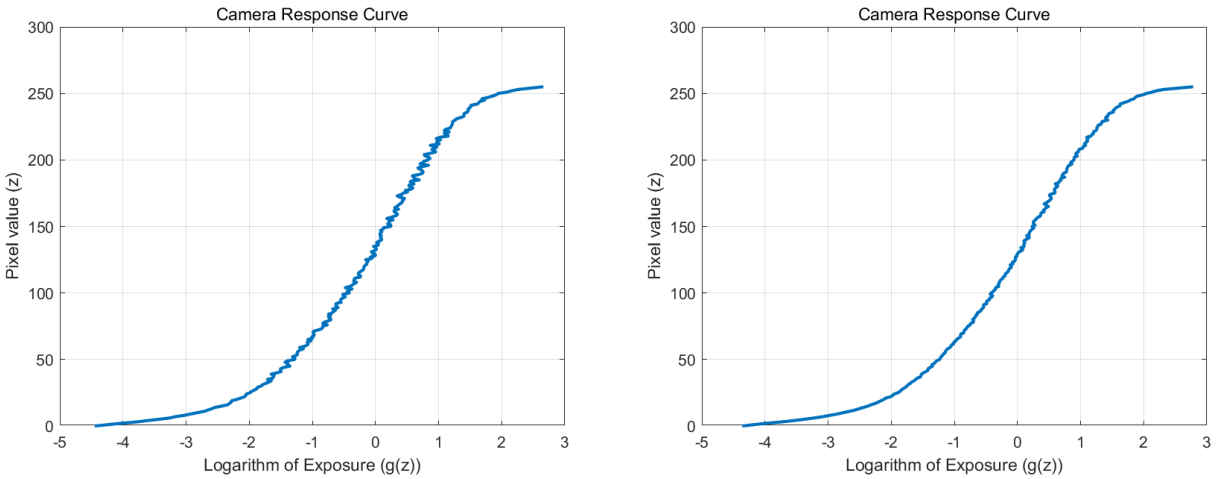

Figure 4: The response curve recovered from figure 3, where the left chooses 1000 pixels and the right chooses 5000.

5.1.2. Optimisation on Scene Arrangements and Sampling

To address the issues mentioned, we must ensure that the selected images have minimal texture and detail to avoid excessive local contrast, which can complicate the recovery of the camera response curve. Additionally, the images should be free of mirror-like reflections, as these can lead to non-linear effects on pixel intensity.

DOI: 10.54254/2753-8818/83/2025.19944

To improve the setup, I created a scene with a lamp and three objects in red, blue, and green, respectively, to cover the full range of exposure for each colour channel. This setup, shown in figure 5, ensures better control over the dynamic range and reduces the complexity in the response curve extraction process.

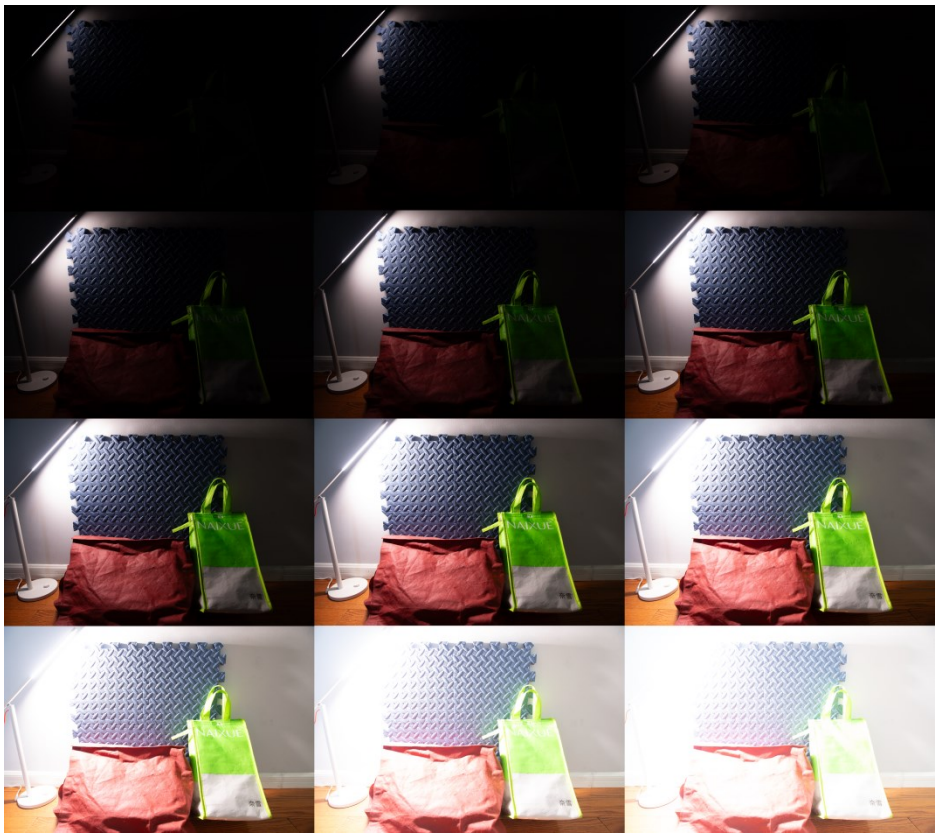

Figure 5: A series of photos taken by Canon EOS 6D Mark2, with exposure times being 4 s, 2 s, 1 s, 1/2 s, 1/4 s, 1/8 s, 1/15 s, 1/30 s, 1/60 s, 1/125 s, 1/250 s, 1/500 s. The selection of exposure times covers the entire dynamic range for this particular scene.

5.1.3. Response curve comparison between two cameras from different brands

In this section, we compare the response curves of two cameras from different brands: the Canon EOS 6D2 and the Sony RX10 IV, with the results shown in figure 6. The curves for the Sony RX10 IV display a slightly steeper slope compared to those of the Canon EOS 6D2. Additionally, the Sony camera reaches a pixel value of 250 at approximately $g(z) = 1.5$, whereas the Canon camera reaches the same value around $g(z) = 3$. This suggests that the Sony RX10 IV is likely more sensitive to light, capturing details in low-light conditions more effectively, while the Canon EOS 6D2 may preserve more detail in highlights. The Canon's requirement for more exposure to achieve maximum brightness suggests it could offer a wider dynamic range in well-lit scenes.

DOI: 10.54254/2753-8818/83/2025.19944

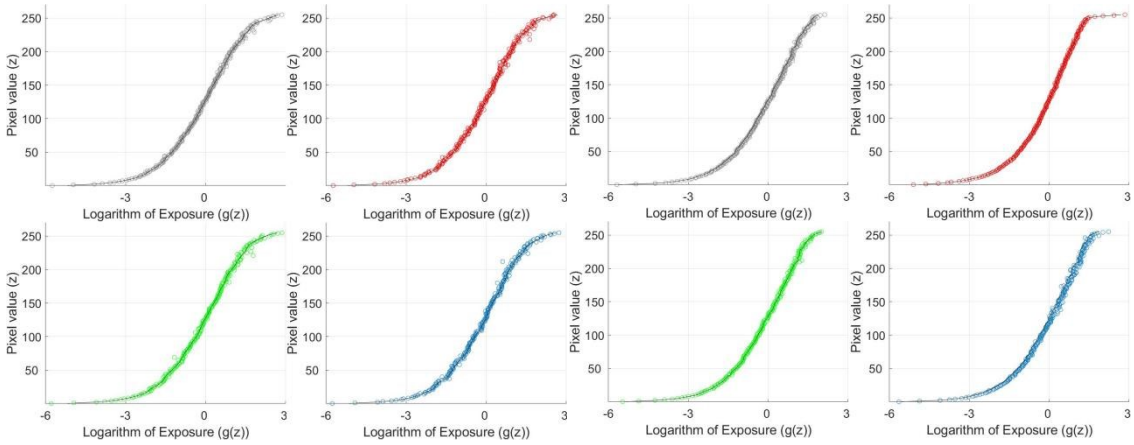

Figure 6: The left response curves are recovered from Canon EOS 6D2 while the right are recovered from SONY Rx10iv. There are four graphs in a image. The four graphs represent the response curve from different channels, where the red curves represents the response curve in red channels, etc.

5.2. HDR Reconstruction

The recovered response curve is then utilised to convert pixel values into radiance values, enabling the creation of an HDR image. This HDR image integrates the information from multiple exposure photographs into a single image, accurately representing the scene's radiance values. By following the procedure discussed earlier, we successfully reconstructed several HDR images, as shown in figure 7.



Figure 7: The left image is the reconstructed HDR image of Figure 5.5 and the right image is the reconstructed image of a cloudy scene with moving winds and a spinning Ferris wheel

Meanwhile, as we know, there are various functions and commercial software available for HDR image reconstruction. To evaluate the effectiveness of different methods, we compare the HDR image reconstructed using the response curve with the image reconstructed using MATLAB's built-in function makehdr(). The results of this comparison are shown in figure 8 and figure 9. This comparison allows us to assess the performance of our custom approach relative to commonly used HDR reconstruction tools.

DOI: 10.54254/2753-8818/83/2025.19944



Figure 8: The image is about a scene of night with many buildings. The left image is reconstructed using the response curve, while the right image is generated using the makehdr() function in MATLAB.

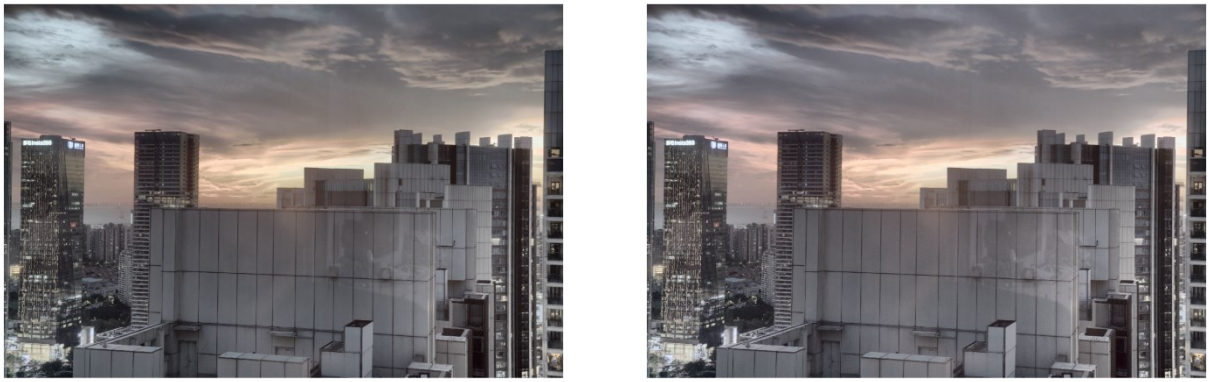

Figure 9: The image is about the scene of sunset with a few constructions. The left image is reconstructed using the response curve, while the right image is generated using the makehdr() function in MATLAB.

From figure 8 and figure 9, we observe notable differences between the HDR images reconstructed using MATLAB's makehdr() function and those generated via the response curve method. Firstly, the image produced by the makehdr() function exhibits noticeably higher colour saturation, which enhances sharpness and contrast. This effect makes the image more visually striking and attractive, commonly used in photography to enhance aesthetic appeal. However, this increased saturation and contrast can compromise the accuracy of the exposure, leading to an exaggerated representation of the scene.

Additionally, in the makehdr()-generated image, some bright areas—particularly in regions of high brightness, such as streetlights or illuminated buildings in night-time scenes—appear overexposed. In contrast, the images reconstructed using the response curve display a more balanced and accurate portrayal in terms of saturation, sharpness, and contrast. The response curve method tends to offer a truer representation of the scene, especially in high dynamic range situations like night-time photography. It effectively prevents overexposure in bright areas, preserving more detail across the image.

In summary, while the makehdr() function might produce visually appealing images with enhanced contrast and saturation, the response curve method delivers better accuracy in exposure and colour representation, making it a more reliable option for realistic imaging.

DOI: 10.54254/2753-8818/83/2025.19944

5.3. Incident Intensity Recovery

To examine that the response curve we recover is accurate, we design an experiment.

5.3.1. Experimental Setup and Procedure

In the experiment, a 650 nm, 5 mW red laser was employed as the light source, and neutral density filters (NDFs) with optical densities (OD) of 1 and 2 to control light intensity. The primary aim of the NDFs is to reduce the intensity of the laser beam in a predictable manner, allowing for precise measurements of pixel values and exposures using the recovered response curve at different intensity levels.

According to the definition of optical density, $OD = -\log_{10}\frac{I_t}{I_0}$, where I_1 is the transmitted intensity and I_0 is the initial intensity, the ratio of exposure between the setups with $OD = 1$ and $OD = 2$ should theoretically be 10. This implies that the light intensity for $OD = 2$ should be one-tenth of the intensity for $OD = 1$. However, since camera sensors do not process exposure in a perfectly linear manner, the pixel values captured by the camera might not reflect this ratio directly. Therefore, we used the response curve to convert pixel values into actual exposures. If the ratio of exposures obtained from the response curve was 10, then the response curve was considered accurate.

The experimental setup is illustrated in figure 10. The laser beam passed through the NDFs and was projected onto the sensor of the camera, which captured images of the light spot. Pixel values of the spot were recorded at various sensor positions (left-top, left-middle, left-bottom, right-top, right-middle, and right-bottom), as shown in figure 11. Images were taken for both $OD = 1$ and $OD = 2$ settings at each position, and the corresponding pixel values were recorded.

By comparing these pixel values and using the response curve to recover the true exposures, we determined whether the ratio between the two exposure levels matched the expected value of 10. This experiment served as a test for the accuracy of the recovered response curve.

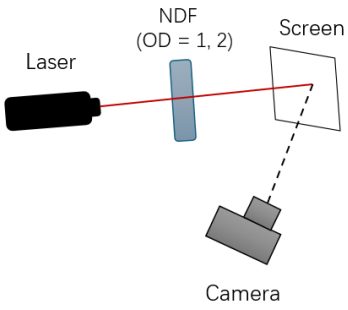

Figure 10: The experimental setup.

5.3.2. Experimental Results

The results of the experiment are presented in figure 1. The table shows the ratio of pixel values recorded at different sensor positions and the corresponding reconstructed incident intensity ratios.

Table 1: The table showcases the pixel value ratios and the actual incident intensity ratio obtained from the response curve at six different positions.

	Pixel Value Ratio	Incident Intensity Ratio
Pixel I (Left-top)	9.000	10.3511

DOI: 10.54254/2753-8818/83/2025.19944

Table 1: (continued).

Pixel II (Left-middle)	9.1667	9.8707
Pixel III (Left-bottom)	9.3333	10.1858
Pixel IV (Right-top)	9.1429	10.2780
Pixel V (Right-middle)	9.2000	10.5303
Pixel VI (Right-bottom)	9.2500	10.1199

The experimental results revealed that the pixel value ratios were slightly less than the expected tenfold ratio. This minor discrepancy is attributed to the non-linear response of the camera sensor. However, after applying the response curve recovery algorithm, the reconstructed incident intensity ratios approximated the expected value of 10. This suggests that the recovery process successfully compensates for the sensor's non-linearity, thus confirming the validity of the recovered response curve.

Despite these positive results, some errors were encountered during the experiment. For example, the laser beam was not perfectly uniform, which could lead to slight variations in the intensity ratios. Additionally, noise and artifacts from the camera itself and the screen's texture in the captured images may have introduced further deviations. Nevertheless, the overall consistency of the recovered intensity ratios across different sensor positions indicates that the recovery process was accurate and effective, providing a reliable approximation of the actual incident light intensity.

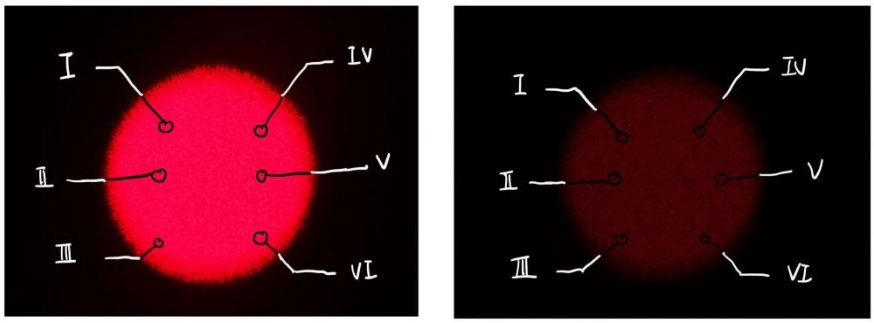

Figure 11: The image shows the original images used to get the ratio and the approximate positions of the chosen pixels

6. Conclusions

In this research, we successfully recovered the non-linear response curve of a DSLR camera and demonstrated its application in high dynamic range (HDR) image reconstruction. By employing the algorithm proposed by Debevec, we recovered the camera's response curve using multiple images taken with different exposure times. This recovered curve enabled us to accurately convert pixel values into relative radiance values, allowing for the reconstruction of HDR images that preserved details in both dark and bright regions of the scene.

The experimental results confirmed the accuracy of the response curve recovery. A comparison between pixel value ratios and actual incident intensity ratios from controlled experiments demonstrated that the recovered response curve effectively compensated for the camera's non-linear response to light. Although minor discrepancies arose due to factors such as non-uniform laser beams

DOI: 10.54254/2753-8818/83/2025.19944

and sensor noise, the overall consistency of the recovered intensity ratios across different sensor positions validated the accuracy of the method.

Additionally, we identified key challenges related to scene selection and pixel sampling, such as the impact of high local contrast and reflective surfaces on response curve recovery. To address these issues, we optimized our scene arrangements by choosing simpler, less reflective objects, which improved the algorithm's performance.

Overall, this investigation underscores the significance of response curve recovery for accurate HDR image reconstruction and incident intensity measurement in DSLR cameras. The methods and findings discussed in this research lay a foundation for future work aimed at enhancing the efficiency and accuracy of response curve recovery algorithms and exploring their applications in other imaging systems.

References

[1] *Glenn D Boreman. Modulation transfer function in optical and electro-optical systems, volume 4. SPIE press Bellingham, Washington, 2001.*

[2] *Gerald C Holst and Terrence S Lomheim. Cmos/ccd sensors. 2011.*

[3] *James Janesick. Lux transfer: Complementary metal oxide semiconductors versus charge-coupled devices. Opt. Eng., 41(6):1203, June 2002.*

[4] *Eric R Fossum. Cmos image sensors: Electronic camera-on-a-chip. IEEE transactions on electron devices, 44(10):1689–1698, 1997.*

[5] *Fil Hunter, Steven Biver, Paul Fuqua, and Robin Reid. Light—science & magic: An introduction to photographic lighting. Routledge, 2021.*

[6] *David D Busch. Digital SLR Cameras and Photography For Dummies. John Wiley & Sons, 2011.*

[7] *Paul E Debevec and Jitendra Malik. Recovering high dynamic range radiance maps from photographs. In Seminal Graphics Papers: Pushing the Boundaries, Volume 2, pages 643–652. 2023.*

[8] *Rafał K Mantiuk, Anna Tomaszewska, and Radosław Mantiuk. Comparison of four subjective methods for image quality assessment. In Computer graphics forum, vol- ume 31, pages 2478–2491. Wiley Online Library, 2012.*

[9] *Phuoc-Hieu Le, Quynh Le, Rang Nguyen, and Binh-Son Hua. Single-image hdr reconstruction by multi-exposure generation. In Proceedings of the IEEE/CVF winter conference on applications of computer vision, pages 4063–4072, 2023.*

[10] *Yu-Lun Liu, Wei-Sheng Lai, Yu-Sheng Chen, Yi-Lung Kao, Ming-Hsuan Yang, Yung- Yu Chuang, and Jia-Bin Huang. Single-image hdr reconstruction by learning to reverse the camera pipeline. In Proceedings of the IEEE/CVF conference on computer vision and pattern recognition, pages 1651–1660, 2020.*

[11] *Su-Kai Chen, Hung-Lin Yen, Yu-Lun Liu, Min-Hung Chen, Hou-Ning Hu, Wen- Hsiao Peng, and Yen-Yu Lin. Learning continuous exposure value representations for single-image hdr reconstruction. In Proceedings of the IEEE/CVF International Conference on Computer Vision, pages 12990–13000, 2023.*

[12] *Erik Reinhard. High dynamic range imaging. In Computer Vision: A Reference Guide, pages 1–6. Springer, 2020.*